AJNR

Glymphatic System Dysfunction in Myelin Oligodendrocyte Glycoprotein Immunoglobulin G Antibody−Associated Disorders: Association with Clinical Disability

Akifumi Hagiwara, Yuji Tomizawa, Yasunobu Hoshino, Kazumasa Yokoyama, Koji Kamagata, Towa Sekine, Kaito Takabayashi, Moto Nakaya, Tomoko Maekawa, Toshiaki Akashi, Akihiko Wada, Toshiaki Taoka, Shinji Naganawa, Nobutaka Hattori and Shigeki Aoki

Glymphatic System Dysfunction in Myelin Oligodendrocyte Glycoprotein Immunoglobulin G Antibody–Associated Disorders: Association with Clinical Disability

Akifumi Hagiwara, Yuji Tomizawa, Yasunobu Hoshino, Kazumasa Yokoyama, Koji Kamagata, Towa Sekine, Kaito Takabayashi, Moto Nakaya, Tomoko Maekawa, Toshiaki Akashi, Akihiko Wada, Toshiaki Taoka, Shinji Naganawa, Nobutaka Hattori, and Shigeki Aoki

ABSTRACT

BACKGROUND AND PURPOSE: Impaired glymphatic function has been suggested to be implicated in the pathophysiology of MS and aquaporin-4 immunoglobulin G-positive neuromyelitis optica spectrum disorder. This study aimed to investigate the interstitial fluid dynamics in the brain in patients with myelin oligodendrocyte glycoprotein antibody disorders (MOGAD), another demyelinating disorder, using a noninvasive imaging technique called the diffusivity along the perivascular space (ALPS) index.

MATERIALS AND METHODS: A prospective study was conducted on 16 patients with MOGAD in remission and 22 age- and sex-matched healthy control subjects. MR imaging was performed using a 3T scanner, and the ALPS index was calculated using diffusion MR imaging data with a b-value of 1000 s/mm^2. The ALPS index and gray matter volumes were compared between the 2 groups, and these parameters were correlated with the Expanded Disability Status Scale.

RESULTS: The mean ALPS index of patients with MOGAD was significantly lower than that of healthy controls (Cohen $d = 0.93$, false discovery rate–corrected $P = .02$). The lower mean ALPS index was significantly associated with a worse Expanded Disability Status Scale score (Spearman $\rho = -0.51$; 95% CI, -0.85 to -0.02; $P = .03$). However, cortical volume and deep gray matter volume were not significantly different between the 2 groups, and they were not correlated with the Expanded Disability Status Scale.

CONCLUSIONS: This study suggests that patients with MOGAD may have impaired glymphatic function, as measured by the ALPS index, which is associated with patient disability. Further study is warranted with a larger sample size.

ABBREVIATIONS: ALPS = diffusivity along the perivascular space; EDSS = Expanded Disability Status Scale; FA = fractional anisotropy; FDR = false discovery rate; IgG = immunoglobulin G; MOG = myelin oligodendrocyte glycoprotein; MOGAD = myelin oligodendrocyte glycoprotein antibody disorders; NMOSD = neuromyelitis optica spectrum disorder; QRAPMASTER = quantification of relaxation times and proton density by multiecho acquisition of a saturation-recovery by using turbo spin-echo readout

Myelin oligodendrocyte glycoprotein antibody disorders (MOGAD) is a newly recognized entity of demyelinating disorders of the CNS defined by the presence of serum immunoglobulin G (IgG) autoantibodies against myelin oligodendrocyte glycoprotein (MOG).[1,2] MOGAD occurs in both children and

adults and is distinct from other neuroinflammatory and demyelinating diseases such as MS or aquaporin-4 IgG-positive neuromyelitis optica spectrum disorder (NMOSD).[3,4] In MOGAD, similar to other demyelinating disorders, breakdown of the BBB and blood-CSF barrier occurs.[5,6] The pathologic hallmark of MOGAD is coexisting perivenous and confluent demyelination with relatively preserved oligodendrocytes.[4,7] A CD4-positive T-cell activation with cytokine release and granulocytic inflammation is typical,[4,7,8] while humoral immunity with complement deposition is occasionally observed.[4,7,9] In addition, the production of reactive oxygen species and the accumulation of iron in the CNS contribute to the disease burden observed in experimental animal models of demyelination.[10,11] A waste-clearing system of the brain may be useful in avoiding further tissue damage due to the accumulation of neurotoxic waste products following inflammatory activity.

While the brain lacks a conventional lymphatic system, recent studies have shown evidence of the existence of a waste-clearance system called the "glymphatic system."[12,13] This system is highly

organized and functions as a fluid transport system, where CSF enters the brain parenchyma and disperses throughout the interstitium via perivascular spaces created by the vascular end-feet of astrocytes. CSF mixes with interstitial fluid, including waste products, and flows through perivenous spaces toward the brain meninges, where it is collected and exported from the CNS via meningeal and cervical lymphatic vessels.[14] The deposition of iron causes impairment of the glymphatic system,[15] which, in turn, leads to the accumulation of reactive oxygen species.[16] The glymphatic system also clears signaling molecules associated with neuroinflammation,[17] and impaired glymphatic function in the presence of neuroinflammation may worsen inflammation by inhibiting the removal of cytokines from the brain.[18]

Despite the increasing interest in the glymphatic system, the lack of noninvasive techniques has hindered the in vivo assessment of its function. Recent studies have used MR imaging to assess glymphatic function, with most using a relatively invasive technique involving the administration of a gadolinium-based contrast agent via intrathecal or IV injection.[19] However, a diffusion-weighted MR imaging technique called diffusivity along the perivascular space (ALPS) has been proposed as a promising noninvasive alternative that does not require the use of tracers.[20,21] ALPS calculates the diffusivity along the deep medullary vein and perivascular space at the level of the lateral ventricle body, providing a measure of perivascular clearance activity in the human brain. A recent study validated the ALPS index as a measure of glymphatic function by correlating it with glymphatic function measurements based on MR imaging after intrathecal administration of a gadolinium-based contrast agent.[22] The ALPS index was found to be lower in various neurologic disorders such as Alzheimer disease[23] and Parkinson disease[24] compared with healthy volunteers. In addition, the ALPS index was also lower in MS and NMOSD than in healthy controls, suggesting an impaired glymphatic system in these demyelinating disorders.[25,26]

Therefore, we hypothesized that the glymphatic system is impaired in patients with MOGAD and contributes to clinical disability by indirectly worsening inflammatory and neurodegenerative processes due to the inefficient removal of soluble waste products, maintaining a proinflammatory state of the brain tissue. We investigated patients with MOGAD using ALPS and correlated the measurements with clinical disability.

MATERIALS AND METHODS
Study Participants
This study was approved by the institutional review board of Juntendo University Hospital, and written informed consent was obtained from all participants. We prospectively recruited 16 patients diagnosed with MOGAD (defined as MOG-antibody positivity using cell-based assays in the context of an acute demyelinating event in patients presenting with a MOGAD phenotype without red flags against a diagnosis of MOGAD, as previously described[2,27]) from March 2018 to February 2022. Disability was assessed using the Expanded Disability Status Scale (EDSS).[28] Patients were consecutively recruited during the remission phase of the disease and had been on stable disease-modifying treatment, oral corticosteroids, or no treatment for at least 3 months and had been free of clinical relapse within the 3 months and IV corticosteroid use within 1 year before MR

imaging. As a control group, we also recruited 22 age- and sex-matched healthy subjects without neurologic and psychological symptoms or a history of neuropsychological disorders. Acquired images were confirmed not to include abnormalities such as moderate-to-severe WM ischemic lesions (Fazekas grade 2 or higher[29]), brain infarction, or tumors.

Image Acquisition and Processing
MR imaging was performed using a 3T scanner (Discovery MR750w; GE Healthcare) with a 19-channel head coil. All participants underwent diffusion MR imaging, 3D T1-weighted imaging, and a 2D axial quantification of relaxation times and proton density by multiecho acquisition of a saturation-recovery by using turbo spin-echo readout (QRAPMASTER) pulse sequence.

Diffusion MR imaging was performed using a single-shot echo-planar imaging sequence along 30 motion-probing gradient directions with $b=1000/mm^2$. In addition, a volume of non-diffusion-weighted images was acquired. The other sequence parameters were the following: TR = 5000 ms, TE = 88.2 ms, FOV = 256 × 256 mm, matrix size = 256 × 256, echo-train length = 128, bandwidth = 1953.12 kHz, section thickness/gap = 4.0/1.0 mm, slices = 30, and acquisition time = 2 minutes 37 seconds. All data sets were visually inspected for artifacts. We corrected in-plane and through-plane distortions of the DWIs caused by eddy currents and motion by using affine brain registration to the non-diffusion-weighted images.[30] Processed images were further denoised using position-orientation adaptive smoothing based on the propagation-separation approach.[31] The fractional anisotropy (FA) map was computed using diffusion data with $b=0$ and 1000 s/mm² by fitting a tensor model. Postprocessing was performed with an in-house program in Matlab (release 2018a; MathWorks).

The acquisition parameters for the 3D T1-weighted images (inversion-recovery spoiled gradient-echo) were as follows: TR = 7.6 ms, TE = 3.09 ms, TI = 400 ms, bandwidth = 244 Hz/pixel, section thickness = 1 mm, FOV = 256 × 256 mm, matrix size = 256 × 256, and acquisition time = 5 minutes 45 seconds.

The QRAPMASTER is a method of acquisition that uses a multislice, multiecho, multisaturation-delay saturation-recovery turbo spin-echo technique to collect images with combinations of 2 TEs and 4 saturation-delay times.[32] We used TEs of 16.9 and 84.5 ms and delay times of 146, 546, 1879, and 3879 ms. The other parameters were as follows: TR = 4.0 seconds, FOV = 240 × 240 mm, matrix = 320 × 320, echo-train length = 10, bandwidth = 31.25 kHz, section thickness/gap = 4.0/1.0 mm, slices = 30, and acquisition time = 7 minutes 12 seconds. The 8 complex images obtained per section were postprocessed using the SyMRI software (Version 8.0; SyntheticMR) to derive longitudinal R1 relaxation and transverse R2 relaxation rates and proton density. Synthetic FLAIR images were created using the R1, R2, and proton density maps with the following postprocessing parameters: TR = 15,000 ms, TE = 100 ms, TI = 3000 ms. An affine transformation was performed to register the acquired images using Statistical Parametric Mapping software (SPM12; http://www.fil.ion.ucl.ac.uk/spm/software/spm12).
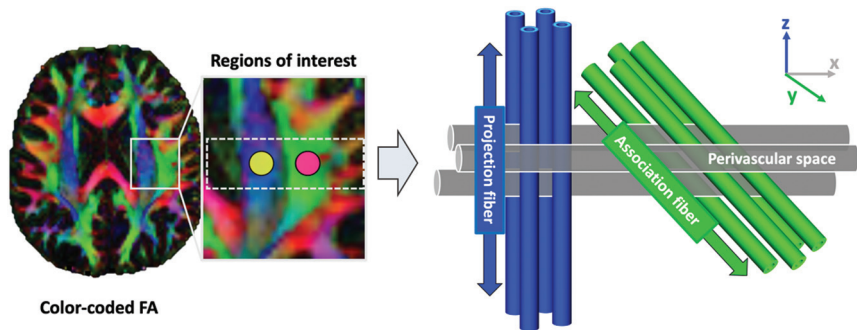
FIG 1. ROI placement for ALPS index calculation. *A*, A color-coded FA map shows the distribution of projection fibers (blue along z-axis) and association fibers (green along y-axis) at the lateral ventricle level. Spherical ROIs with a 5-mm diameter were placed in the projection and association areas. *B*, A schematic illustration of the relationship between the principal fiber and perivascular spaces, with the perivascular space running parallel to the medullary vein and perpendicular to the projection and association fibers.

Demographic characteristics of the participants

	Healthy Controls	MOGAD	P Value
No.	22	16	NA
Age (mean) (yr)[a]	44.77 (SD, 14.58)	44.19 (SD, 17.93)	.94
Sex (male/female)[b]	6:16	4:12	.88
Disease duration (mean) (yr)	NA	8.06 (SD, 11.86)	NA
EDSS (median) (range)	NA	0 (0–7)	NA
WM lesion, (mean) (mL)	NA	8.81 (SD, 7.67)	NA

Note:— NA indicates not applicable.
[a] The statistical analysis was performed with a *t* test.
[b] The statistical analysis was performed with a χ^2 test.

the native color-coded FA map of the participant with the least warping (ie, the smallest sum of squared differences) (Fig 1). The ROIs were registered to the standard space image and then to the FA map of each participant. The position of the ROI was manually verified by referring to the lesion map. If the ROI overlapped with a lesion, the position of the ROI was manually shifted to avoid overlap while ensuring that the 2 ROIs were placed perpendicular to the lateral ventricles. This step is important because the perpendicular alignment between the perivascular space and nerve fiber direction adjacent to the lateral ventricles may be disrupted due to demyelination.[25]

Finally, the ALPS index was calculated as the mean of the x-axis diffusivity in the projection area ($D_{xx,proj}$) and x-axis diffusivity in the association area ($D_{xx,assoc}$), divided by the mean of the y-axis diffusivity in the projection area ($D_{yy,proj}$) and the z-axis diffusivity in the association area ($D_{zz,assoc}$) as follows:

$$ALPS\ index = \frac{Mean\ (D_{xx,proj}, D_{xx,assoc})}{Mean\ (D_{yy,proj}, D_{zz,assoc})}.$$

Lesion Maps

For all patients, hyperintense lesions were automatically segmented on synthetic FLAIR images by using the lesion-prediction algorithm[33] implemented in the Lesion Segmentation Toolbox (Version 2.0.15; https://www.applied-statistics.de/lst.html)[34] running in SPM12. All lesion maps were visually inspected and manually corrected by an expert neuroradiologist (A.H.) with 12 years of experience. The whole-brain WM lesion volume in each patient was calculated by multiplying the lesion area by the section thickness.

Brain Volumes

Before segmentation and volume calculation, the Lesion Segmentation Toolbox was used to fill the WM lesions detected on FLAIR images for the 3D T1-weighted images. The cortex and subcortical gray matter were segmented using FreeSurfer (Version 6.0; http://surfer.nmr.mgh.harvard.edu)[35] and the FMRIB Software Library (Version 6.0.0; http://www.fmrib.ox.ac.uk/fsl),[36] respectively. These segmentation masks were used to calculate the cortical volume and subcortical gray matter volume for each participant.

Calculation of the ALPS Index

The ALPS index was calculated from the DWI data using a semi-automated pipeline developed and validated by Taoka et al.[37] The FA maps of all participants were registered to a FMRIB58_FA standard space image (https://fsl.fmrib.ox.ac.uk/fsl/fslwiki/FMRIB58_FA) through linear and nonlinear transformations. Spherical ROIs of 5-mm diameter were placed in the projection and association fiber areas at the level of the lateral ventricle bodies in both hemispheres using

The left and right ALPS indices were then averaged and used for statistical analysis. An ALPS index close to 1.0 suggests minimal diffusivity along the perivascular space, while a higher value indicates increased diffusivity.

Statistical Analysis

Demographic variables for patients with MOGAD and healthy controls were compared using a *t* test or χ^2 test as appropriate. Structural MR imaging metrics and the mean ALPS index were compared between patients with MOGAD and healthy controls using a *t* test, with false discovery rate (FDR) correction applied to consider multiple comparisons of these MR imaging metrics. Cohen *d* effect sizes of the group differences were calculated. The Spearman rank correlation test was used to investigate the associations of MR imaging measurements in patients with MOGAD with EDSS scores and disease duration. Matlab was used for statistical analyses, with statistical significance set at $P < .05$.

RESULTS

The demographic characteristics of the healthy control group and patients with MOGAD are presented in the Table. There were no significant differences in age and sex between the 2 groups. Of the 16 patients with MOGAD, 14 were receiving chronic oral steroids, while none were on disease-modifying treatments.

Figure 2 displays violin and box plots comparing the MR imaging metrics of the MOGAD and healthy control groups. There was no patient with MOGAD who required manual correction of an ROI to avoid a WM lesion. The mean ALPS index
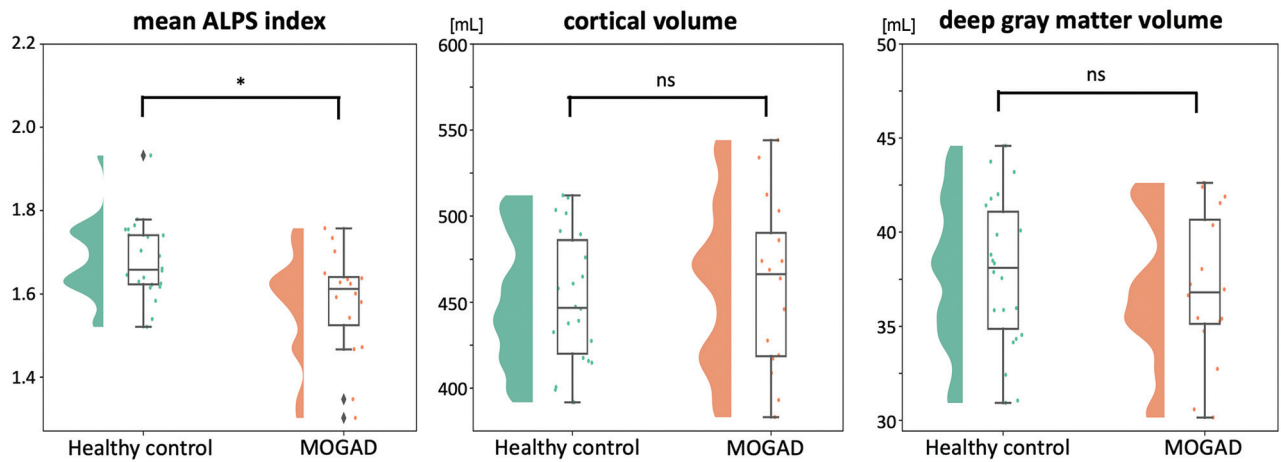
FIG 2. Violin and box plots of the MR imaging metrics compared between the MOGAD and healthy control groups. The *asterisk* indicates FDR-corrected *P* < .05; ns, indicates no significance.
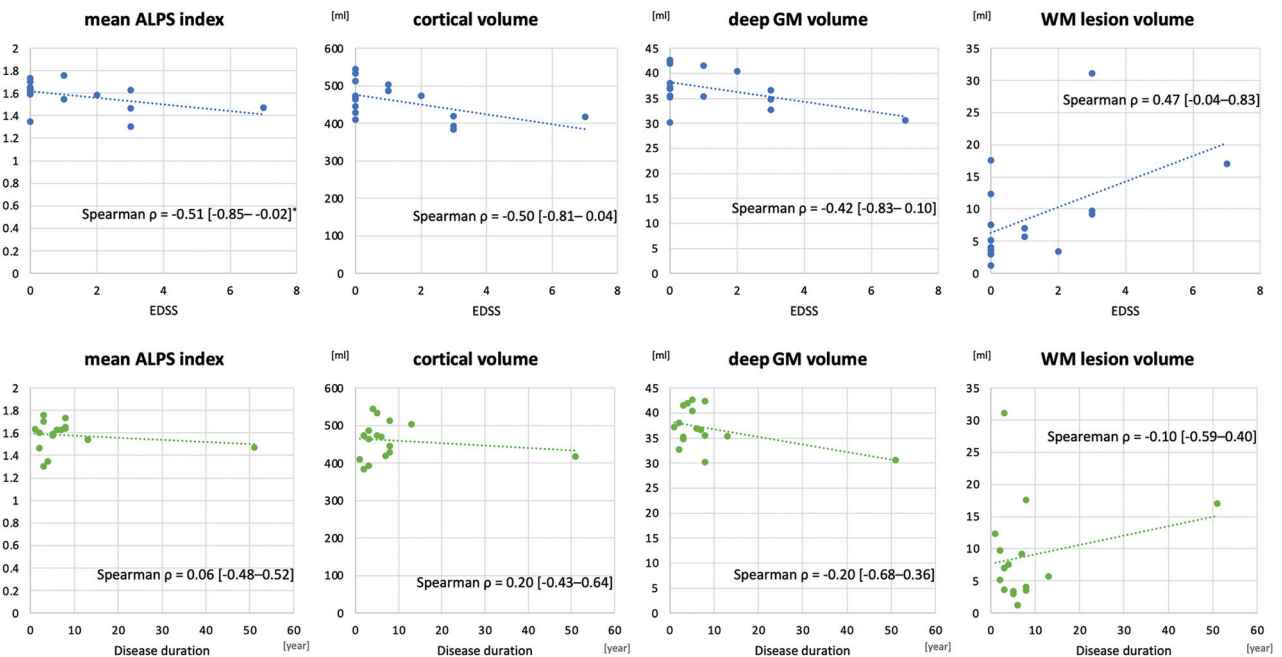
FIG 3. Scatterplots are presented to show the correlations between clinical characteristics and MR imaging metrics. An *asterisk* indicates statistical significance at *P* < .05.

DISCUSSION

of the patients with MOGAD was significantly lower than that of the control group (1.58 [SD, 0.13] versus 1.68 [SD, 0.09], FDR-corrected *P* = .02, Cohen *d* = 0.93). However, cortical volume and deep gray matter volume did not differ significantly between patients with MOGAD and healthy controls (459.68 [SD, 49.01] mL versus 451.73 [SD, 37.97] mL, FDR-corrected *P* = .58, Cohen *d* = 0.19; 37.00 [SD, 3.97] mL versus 37.86 [SD, 4.00] mL, FDR-corrected *P* = .58, Cohen *d* = 0.21). Moreover, the mean ALPS index of the patients with MOGAD was significantly negatively correlated with EDSS ($\rho = -0.51$; 95% CI, −0.85 to −0.02; *P* = .03) but not with disease duration ($\rho = 0.06$; 95% CI, −0.48−0.52, *P* = .67) (Fig 3). Cortical volume and WM lesion volume were not significantly correlated with EDSS or disease duration.

In the current study, we investigated the function of the interstitial fluid dynamics in patients with MOGAD in remission, using a noninvasive MR imaging metric called the ALPS index, which measures diffusivity along the perivascular space. Our results showed that the ALPS index was significantly lower in patients with MOGAD compared with healthy controls, indicating reduced interstitial fluid dynamics, which may suggest impaired glymphatic system function in MOGAD. Additionally, we found a significant correlation between the ALPS index in patients with MOGAD and their clinical disability.

Impaired interstitial fluid dynamics, as indicated by a decreased ALPS index, has also been reported in other neuroinflammatory diseases, namely MS and NMOSD.[25,26] Like our study, these

previous studies investigated patients during their relapse-free phase. Neuroinflammation can impede the process of vascular polarization of aquaporin-4 from the astrocytic end-feet toward the soma due to abnormal localization of aquaporin-4, ultimately resulting in a reduction in glymphatic flow.[17] Several studies have demonstrated that conditions associated with chronic neuroinflammation can sustain this decreased glymphatic flow.[38-40] Additionally during inflammation, immune cells that infiltrate the perivascular spaces are known to accumulate, potentially obstructing the flow of fluid around the blood vessels and impeding the influx of CSF.[41-43] This disruption in glymphatic flow, along with the resulting buildup of cytokines and metabolic wastes, may contribute to a harmful cycle that perpetuates neuroinflammation.[44] Previous damage to the glymphatic system during the attack phase, ongoing inflammation and neurodegeneration, or both can be possible causes of the decreased ALPS index in demyelinating disorders, including MOGAD investigated in the current study.

A previous study demonstrated lower cortical and deep gray matter volumes in patients with MOGAD compared with healthy controls,[45] while the current study did not show a statistically significant difference. Additionally, the previous study showed a significant negative correlation between deep gray matter volume and the EDSS score, which was not observed in the current study. These discrepancies could be due to the smaller sample size of the current study. However, the current study found a significant difference in the ALPS index between patients with MOGAD and healthy controls, as well as a significant negative correlation between the index and EDSS scores. Therefore, the ALPS index may be a more sensitive biomarker for reflecting the disease process of MOGAD than brain volumes. The causative role of glymphatic dysfunction in patient disability should be investigated through longitudinal studies. Such studies may eventually evaluate the potential of glymphatic function assessment as a predictive marker of relapse and disease progression.

In MS, the ALPS index showed a correlation with disease duration, whereas in NMOSD and MOGAD, it did not. This finding may suggest an early glymphatic function impairment in NMOSD and MOGAD, which could be linked to the pathophysiology of the diseases, because these 2 disorders rarely have a progressive disease course.[2] In these disorders, the severity of clinical manifestations is likely to be influenced by the magnitude of the pathogenic mechanism, irrespective of the disease duration.

There are some limitations to the current study. First, the sample size was small. A further study is warranted with a larger sample size to confirm our findings. Second, the ALPS index is limited in its ability to assess glymphatic function throughout the entire brain due to its reliance on the geometric relationship between projection and association fibers and medullary arteries and veins in the lateral ventricle body.[20,46] Therefore, the ALPS index can be evaluated only at the lateral ventricle body level. Additionally, the ALPS index does not exclusively measure the diffusivity of the perivenous space surrounding the deep medullary vein but is also affected by the surrounding WM microstructure within the ROI. Also, the timescale of the measurement by the ALPS index is much shorter than the actual rate of flow for glymphatic clearance.[47] Hence, careful interpretation and further investigation of the ALPS index are necessary. Furthermore, we did not use gadolinium-based contrast agents to measure glymphatic function in our study. While the use of CSF tracers is rather invasive, it is currently considered the criterion standard for assessing glymphatic function.[46] However, the ALPS index has shown a high correlation with glymphatic function measures obtained through MR imaging with administration of an intrathecal gadolinium-based contrast agent.[22]

CONCLUSIONS

We used the ALPS index, a noninvasive method, to assess the function of the glymphatic system. We demonstrated that patients with MOGAD exhibit impaired glymphatic function and that reduced glymphatic function is linked to patient disability. The findings of this study could potentially enhance our understanding of the pathophysiology of MOGAD and contribute to the development of new therapeutic strategies.

REFERENCES

1. Reindl M, Schanda K, Woodhall M, et al. **International multicenter examination of MOG antibody assays.** *Neurol Neuroimmunol Neuroinflamm* 2020;7:e674 CrossRef Medline
2. Banwell B, Bennett JL, Marignier R, et al. **Diagnosis of myelin oligodendrocyte glycoprotein antibody-associated disease: International MOGAD Panel proposed criteria.** *Lancet Neurol* 2023;22:268–82 CrossRef Medline
3. Kim H, Lee EJ, Kim S, et al. **Serum biomarkers in myelin oligodendrocyte glycoprotein antibody-associated disease.** *Neurol Neuroimmunol Neuroinflamm* 2020;7:e708 CrossRef
4. Höftberger R, Guo Y, Flanagan EP, et al. **The pathology of central nervous system inflammatory demyelinating disease accompanying myelin oligodendrocyte glycoprotein autoantibody.** *Acta Neuropathol* 2020;139:875–92 CrossRef Medline
5. Tanaka S, Hashimoto B, Izaki S, et al. **Clinical and immunological differences between MOG associated disease and anti AQP4 antibody-positive neuromyelitis optica spectrum disorders: blood–brain barrier breakdown and peripheral plasmablasts.** *Mult Scler Relat Disord* 2020;41:102005 CrossRef Medline
6. Jarius S, Pellkofer H, Siebert N, et al; in cooperation with the Neuromyelitis Optica Study Group (NEMOS). **Cerebrospinal fluid findings in patients with myelin oligodendrocyte glycoprotein (MOG) antibodies, Part 1: results from 163 lumbar punctures in 100 adult patients.** *J Neuroinflammation* 2020;17:261 CrossRef Medline
7. Takai Y, Misu T, Kaneko K, et al; Japan MOG-antibody Disease Consortium. **Myelin oligodendrocyte glycoprotein antibody-associated disease: an immunopathological study.** *Brain* 2020;143:1431–46 CrossRef Medline
8. Kaneko K, Sato DK, Nakashima I, et al. **CSF cytokine profile in MOG-IgG neurological disease is similar to AQP4-IgG NMOSD but distinct from MS: a cross-sectional study and potential therapeutic implications.** *J Neurol Neurosurg Psychiatry* 2018;89:927–36 CrossRef Medline
9. Jarius S, Metz I, König FB, et al. **Screening for MOG-IgG and 27 other anti-glial and anti-neuronal autoantibodies in 'pattern II multiple sclerosis' and brain biopsy findings in a MOG-IgG-positive case.** *Mult Scler* 2016;22:1541–49 CrossRef Medline
10. Zarruk JG, Berard JL, Passos dos Santos R, et al. **Expression of iron homeostasis proteins in the spinal cord in experimental autoimmune encephalomyelitis and their implications for iron accumulation.** *Neurobiol Dis* 2015;81:93–107 CrossRef Medline

11. Ruuls SR, Bauer J, Sontrop K, et al. **Reactive oxygen species are involved in the pathogenesis of experimental allergic encephalomyelitis in Lewis rats**. *J Neuroimmunol* 1995;56:207–17 CrossRef Medline

12. Iliff JJ, Wang M, Liao Y, et al. **A paravascular pathway facilitates CSF flow through the brain parenchyma and the clearance of interstitial solutes, including amyloid β**. *Sci Transl Med* 2012;4:147ra111 CrossRef Medline

13. Lohela TJ, Lilius TO, Nedergaard M. **The glymphatic system: implications for drugs for central nervous system diseases**. *Nat Rev Drug Discov* 2022;21:763–79 CrossRef Medline

14. Nedergaard M, Goldman SA. **Glymphatic failure as a final common pathway to dementia**. *Science* 2020;370:50–56 CrossRef Medline

15. Liang S, Lu Y, Li Z, et al. **Iron aggravates the depressive phenotype of stressed mice by compromising the glymphatic system**. *Neurosci Bull* 2020;36:1542–46 CrossRef Medline

16. Gu S, Li Y, Jiang Y, et al. **Glymphatic dysfunction induced oxidative stress and neuro-inflammation in major depression disorders**. *Antioxidants (Basel)* 2022;11:2296 CrossRef Medline

17. Mogensen FL, Delle C, Nedergaard M. **The glymphatic system (en) during inflammation**. *Int J Mol Sci* 2021;22:7491 CrossRef Medline

18. Filiano AJ, Gadani SP, Kipnis J. **How and why do T cells and their derived cytokines affect the injured and healthy brain?** *Nat Rev Neurosci* 2017;18:375–84 CrossRef Medline

19. Naganawa S, Taoka T. **The glymphatic system: a review of the challenges in visualizing its structure and function with MR imaging**. *Magn Reson Med Sci* 2022;21:182–94 CrossRef Medline

20. Taoka T, Masutani Y, Kawai H, et al. **Evaluation of glymphatic system activity with the diffusion MR technique: diffusion tensor image analysis along the perivascular space (DTI-ALPS) in Alzheimer's disease cases**. *Jpn J Radiol* 2017;35:172–78 CrossRef Medline

21. Taoka T, Ito R, Nakamichi R, et al. **Diffusion-weighted image analysis along the perivascular space (DWI-ALPS) for evaluating interstitial fluid status: age dependence in normal subjects**. *Jpn J Radiol* 2022;40:894–902 CrossRef Medline

22. Zhang W, Zhou Y, Wang J, et al. **Glymphatic clearance function in patients with cerebral small vessel disease**. *NeuroImage* 2021;238:118257 CrossRef Medline

23. Kamagata K, Andica C, Takabayashi K, et al; for the Alzheimer's Disease Neuroimaging Initiative. **Association of MRI indices of glymphatic system with amyloid deposition and cognition in mild cognitive impairment and Alzheimer disease**. *Neurology* 2022;99:e2648–60 CrossRef Medline

24. Chen HL, Chen PC, Lu CH, et al. **Associations among cognitive functions, plasma DNA, and diffusion tensor image along the perivascular space (DTI-ALPS) in patients with Parkinson's disease**. *Oxidative Medicine and Cellular Longevity* 2021;2021:1–10.

25. Carotenuto A, Cacciaguerra L, Pagani E, et al. **Glymphatic system impairment in multiple sclerosis: relation with brain damage and disability**. *Brain* 2022;145:2785–95 CrossRef Medline

26. Cacciaguerra L, Carotenuto A, Pagani E, et al. **Magnetic resonance imaging evaluation of perivascular space abnormalities in neuromyelitis optica**. *Ann Neurol* 2022;92:173–83 CrossRef Medline

27. Marignier R, Hacohen Y, Cobo-Calvo A, et al. **Myelin-oligodendrocyte glycoprotein antibody-associated disease**. *Lancet Neurol* 2021;20:762–72 CrossRef Medline

28. Kurtzke JF. **A new scale for evaluating disability in multiple sclerosis**. *Neurology* 1955;5:580–83 CrossRef Medline

29. Fazekas F, Chawluk JB, Alavi A, et al. **MR signal abnormalities at 1.5 T in Alzheimer's dementia and normal aging**. *AJR Am J Roentgenol* 1987;149:351–56 CrossRef Medline

30. Mohammadi S, Möller HE, Kugel H, et al. **Correcting eddy current and motion effects by affine whole-brain registrations: evaluation of three-dimensional distortions and comparison with slicewise correction**. *Magn Reson Med* 2010;64:1047–56 CrossRef Medline

31. Becker SM, Tabelow K, Voss HU, et al. **Position-orientation adaptive smoothing of diffusion weighted magnetic resonance data (POAS)**. *Med Image Anal* 2012;16:1142–55 CrossRef Medline

32. Hagiwara A, Warntjes M, Hori M, et al. **SyMRI of the brain: rapid quantification of relaxation rates and proton density, with synthetic MRI, automatic brain segmentation, and myelin measurement**. *Invest Radiol* 2017;52:647–57 CrossRef Medline

33. Egger C, Opfer R, Wang C, et al. **MRI FLAIR lesion segmentation in multiple sclerosis: does automated segmentation hold up with manual annotation?** *Neuroimage Clin* 2017;13:264–70 CrossRef Medline

34. Schmidt P, Gaser C, Arsic M, et al. **An automated tool for detection of FLAIR-hyperintense white-matter lesions in multiple sclerosis**. *Neuroimage* 2012;59:3774–83 CrossRef Medline

35. Fischl B. **FreeSurfer**. *Neuroimage* 2012;62:774–81 CrossRef Medline

36. Patenaude B, Smith SM, Kennedy DN, et al. **A Bayesian model of shape and appearance for subcortical brain segmentation**. *Neuroimage* 2011;56:907–22 CrossRef Medline

37. Taoka T, Ito R, Nakamichi R, et al. **Reproducibility of diffusion tensor image analysis along the perivascular space (DTI-ALPS) for evaluating interstitial fluid diffusivity and glymphatic function: CHanges in Alps index on Multiple conditiON acquIsition eXperiment (CHAMONIX) study**. *Jpn J Radiol* 2022;40:147–58 CrossRef Medline

38. Kress BT, Iliff JJ, Xia M, et al. **Impairment of paravascular clearance pathways in the aging brain**. *Ann Neurol* 2014;76:845–61 CrossRef Medline

39. Ren Z, Iliff JJ, Yang L, et al. **'Hit & Run' model of closed-skull traumatic brain injury (TBI) reveals complex patterns of post-traumatic AQP4 dysregulation**. *J Cereb Blood Flow Metab* 2013;33:834–45 CrossRef Medline

40. Wang M, Iliff JJ, Liao Y, et al. **Cognitive deficits and delayed neuronal loss in a mouse model of multiple microinfarcts**. *J Neurosci* 2012;32:17948–60 CrossRef Medline

41. Rustenhoven J, Drieu A, Mamuladze T, et al. **Functional characterization of the dural sinuses as a neuroimmune interface**. *Cell* 2021;184:1000–16.e27 CrossRef Medline

42. Ivan DC, Walthert S, Berve K, et al. **Dwellers and trespassers: mononuclear phagocytes at the borders of the central nervous system**. *Front Immunol* 2020;11:609921 CrossRef Medline

43. Zhou H, Andonegui G, Wong CHY, et al. **Role of endothelial TLR4 for neutrophil recruitment into central nervous system microvessels in systemic inflammation**. *J Immunol* 2009;183:5244–50 CrossRef Medline

44. Salvador AF, de Lima KA, Kipnis J. **Neuromodulation by the immune system: a focus on cytokines**. *Nat Rev Immunol* 2021;21:526–41 CrossRef Medline

45. Duan Y, Zhuo Z, Li H, et al. **Brain structural alterations in MOG antibody diseases: a comparative study with AQP4 seropositive NMOSD and MS**. *J Neurol Neurosurg Psychiatry* 2021;92:709–16 CrossRef Medline

46. Naganawa S, Taoka T, Ito R, et al. **The glymphatic system in humans: investigations with magnetic resonance imaging**. *Invest Radiol* 2023 Mar 13 [Epub ahead of print] CrossRef

47. Pla V, Bork P, Harnpramukkul A, et al. **A real-time in vivo clearance assay for quantification of glymphatic efflux**. *Cell Rep* 2022;40:111320 CrossRef Medline